utomated Vibrational Design and Natural Frequency Tuning of Multi-Material Structures

Nicholas Cheney, Ethan Ritz, Hod Lipson
Creative Machines Lab
Cornell University
Ithaca, NY
nac93@cornell.edu, etr38@cornell.edu, hod.lipson@cornell.edu

BSTR CT

Natural frequency tuning is a vital engineering problem. Every structure has natural frequencies, where vibrational loading at nearby frequencies excite the structure. This causes the structure to resonate, oscillating until energy is dissipated through friction or structural failure. Examples of fragility and distress from vibrational loading include civil structures during earthquakes or aircraft rotor blades. Tuning the structure's natural frequencies away from these vibrations increases the structure's robustness. Conversely, tuning towards the frequencies caused by vibrations can channel power into energy harvesting systems. Despite its importance, natural frequency tuning is often performed adhoc, by attaching external vibrational absorbers to a structure. This is usually adequate only for the lowest ("fundamental") resonant frequencies, yet remains standard practice due to the unintuitive and difficult nature of the problem. Given Evolutionary Algorithms' (EA's) ability to solve these types of problems, we propose to approach this problem with the EA CPPN-NEAT to evolve multi-material structures which resonate at multiple desired natural frequencies without external damping. The EA assigns the material type of each voxel within the discretized space of the object's existing topology, preserving the object's shape and using only its material composition to shape its frequency response.

Categories and Subject Descriptors: J.6 [**Computer-Aided Engineering**]:Computer-aided design
General Terms: Algorithms, Design, Experimentation
Keywords: Genetic Algorithms, Design Automation, Frequency Tuning, Vibration Analysis, Structural Optimization

1. INTRODUCTION

In engineering mechanics, the response of a structure to vibrational loads is of acute interest and importance. Every object will exhibit some motion when excited with any periodic load – such as vibrations. But vibrations at certain frequencies will excite certain objects with greater intensity. The natural frequencies of each object dictate the frequencies of vibrations which exhibit particularly intense responses. In many cases, this type of loading is harmful to the system – larger responses put more stress on the structure. The energy trapped in the structure through these oscillating motions is not efficiently dissipated into the surrounding environment in these cases, leading to weakening or even failure over time (Fig. 1).

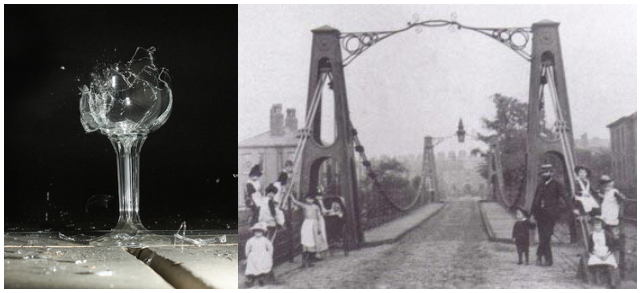

Figure 1: *left)* **Resonant vibrations are a common source of fragility in natural objects. Here a glass fails in the presence of an acoustic wave at resonance.** *right)* **On a larger scale, structural failure through periodic loading of the Broughton Suspension Bridge caused its collapse in 1831 due to the resonance of the solders marching in lockstep [14].**

Large arch dams in earthquake prone areas are one example of antagonistic periodic loading, where oscillations at resonance encourage cracking and rupture through brittle concrete [1]. Wind turbine blades are another instance of this, where rotation at a resonant frequency may cause tip deflection that stresses the blades and lowers their e ectiveness [15]. In aerospace applications, or other vehicles producing massive propulsive loads, the vibrations caused can be particularly damaging [6].

On the other hand, some applications may benefit from increased oscillatory response. Oscillations of larger magnitude contain more energy, which are ideal for power harvesting mechanisms such as microelectromechanical systems (MEMS) like piezoelectric microcantilevers. In this case, the lack of energy dissipation from structures with resonant frequencies close to the frequency of the vibrations enhances the efficiency of these energy harvesting systems [3, 22].

However, the process of tuning structures to have specific resonant frequencies remains largely unintuitive – changes to the material properties at one point in a structure often lead

GE O'14, July 12-16, 2014, Vancouver, BC, Canada.

to non-linear e ects on its vibrational response, both near and far from the point of change. Thus existing methods usually change the shape of the structure, often involving the addition of mass dampers to the system or requiring significant structural modifications. In cases where weight and size are at a premium, such as aerospace or remote sensing, these solutions are unsatisfying. Additionally, many of these damping strategies are only useful for the first ("fundamental") resonant frequency.

In many cases, important structures must interface into a pre-existing system, be robust (free from fragile additions), or serve aesthetic purposes. In existing structures the topology has often already been optimized, such as airfoils tuned for aerodynamic efficiency. In these cases, it would be advantageous to perform vibrational optimization of structures which preserves the overall shape of the object while also giving it desirable vibrational properties.

Muti-material design involves the use of di erent material types within a given shape to produce overall object properties outside of those available to the given shape composed of a single material. By optimizing a structure's vibrational response though multi-material design within an existing envelope, we open new doors towards the study and implementation of vibrational optimization of these fixed topology structures. Additionally, with current advances in multi-material additive manufacturing, we now have the ability to specify the placement and interwovenness of individual material droplets with vastly di erent properties during the manufacturing of a given structure, making such designs physically realizable today.

In this study, we optimize the two dimensional projection of a fixed-free cantilevered beam, with the first ten natural frequencies optimized to reproduce a randomly chosen resonant frequency profile. This is a particularly difficult and unintuitive problem because the material properties at each voxel are coupled (often non-linearly, and non-locally) with the material properties at every other voxel to produce the vibrational response of the object as a whole. Furthermore, this static topology responds di erently to vibrations at different frequencies, making ad-hoc tuning of more than one or two natural frequencies exceptionally challenging.

Due to the unintuitive nature of the problem, we use evolutionary computation to traverse this design space – specifically the evolutionary algorithm CPPN-NEAT. We choose this because the Compositional Pattern Producing Network (CPPN) genome provides a compact and evolvable representation of the discretized physical design space necessary for this problem. We use this EA to optimize the placement of two materials (sti and soft) at each discretized voxel of the structure's original shape envelope. We optimize towards randomly chosen frequency profiles (which specify the first ten natural frequencies of a structure), and show the promise of this approach to become an automated design platform for structural vibration optimization going forward.

2. B CKGROUND

Controlling system performance through the frequency domain is a classical idea [18], but conventional engineering strategies have remained largely unchanged since the early 20th century. In many cases, harmful vibrations are attenuated by directing energy away from the most sensitive parts of the system, to another auxiliary system. This is done through the addition of tuned vibrational absorbers (TVA) [17, 25, 26]. However these systems come with the tradeo of increasing the mass and complexity of the original structure. This typically involves augmenting the system with spring-mass element or small cantilever with a first resonant frequency tuned to that of the undesired excitation, where the undesirable energy is contained within oscillations of this auxiliary structure until it is dissipated though friction.

This process is not only inefficient, but fails to fully explore the design space - as the attachment location and parameters of these devices are often chosen through intuition and physical guess-and-check iterations by the engineers, and are thus biased by the engineer's assumptions and training. Additionally, the amount of energy that can be absorbed by these types of systems is limited. As the TVA becomes large, its own dynamics begin coupling with the original system. This not only produces harmful vibrations within the original structures, but also changes its resonance profile and further complicates design. Furthermore, volume constraints of the system, such as inside the fairing of a rocket in launch, inherently restrict the size and shape of a TVA.

Some work has examined changing the system's topology to have a desired frequency profile without the addition of other components. Many of these strategies optimize the placement or parameter settings of a few predetermined basic structures, such as rods or trusses [13, 23, 7]. Duhring et al. studied the automatic design of structures with desired natural frequencies using homogenization [10]. However, this method could only optimize for a single frequency band, trying to maximize or minimize the frequency response between a set of frequency borders. This strategy also involved the generation of structures with complex and unpredictable shapes, rather than optimizing the response of an existing structure's topology. Du and Olho used topological optimization to automate the design of a voxelized plate structure with a binary material array to minimize sound power flow [9]. However, their designs were also constrained to the optimization of just a single frequency.

Our system expands upon these strategies by allowing us to optimize an arbitrarily large number of natural frequencies of a structure. Additionally, any number of material values can be used for any geometry. Since our search of the design space is topology-preserving; the final product will still have the shape of the original design, ensuring it will have the same functionality and maintain previous topology optimization, with only natural frequencies changed.

3. METHODS

Our method involves tuning the natural frequencies of a structure, which for lightly damped systems well approximates the resonant frequencies (where vibrational energy resonates to create sustained oscillations). First, the user specifies a design geometry. In many practical cases this is a pre-existing object shape, in this study we simply use a 2D projection of a cantilever beam, fixed on one end. Next the user produces a list of n desired natural frequencies. These frequencies are again dependent on the specific application; vibration in the environment can be found by measuring excitation loads with an accelerometer and applying the Discrete Fourier Transform [8]. Here, we select the frequency profile randomly (Sec. 3.4). Finally a selection of materials from which to construct the object is necessary. These depend on the additive manufacturing capabilities and supplies

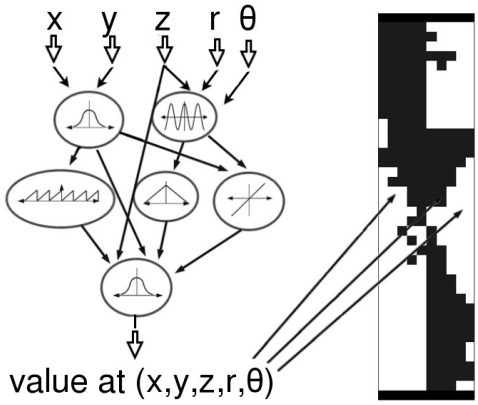

Figure 2: The CPPN genome iterates through each voxel in the discretized design space, placing either a soft or sti voxel at each location to produce the phenotype structure it encodes (Sec. 3.2)

available to the user, and in this case is simply represented by two idealized materials, one an order of magnitude sti er than the other. The structure to be optimized is meshed in a uniform voxelized grid. In this study, the beam is discretized into a 40x10x1 set of uniform cubic voxels. Each of these voxels is assigned a material according to the phenotype described by its associated Compositional Pattern Producing Network (CPPN) genome (Sec. 3.2). The natural frequencies of the structure are calculated (Sec. 3.1), and used to determine the individual's fitness (Sec. 3.3). Individuals who best minimize the error between the calculated and desired natural frequency profile are disproportionally favored to reproduce (and are subject to both genetic mutations and crossover in this process), creating the next generation to again iterative this evolutionary process.

3.1 pproximating Natural Frequencies with FEM

Determining the harmonic behavior of an object is equivalent to solving for the eigenvalues of the matrix representing the FEM mesh of the structure. The shape and material of the system will govern the frequency at which each of the n desired natural frequencies lie. There is one natural frequency per degree of freedom of the system, but typically the number of nodes required for accurate simulation far exceeds the number of natural frequencies in an engineering range of interest. In this case of the 40x10 discretized voxels, the 400 voxels are approximated by 1301 nodes, with 8 nodes per quadrilateral element (many nodes are shared between adjacent elements). This is more than adequate to approximate the first 10 natural frequencies. These are computed using a generalized conjugate residual method, to a residual error $< 10^{-8}$. For this computation we employ Elmer, a popular open source finite element software for multiphysical problems, developed and maintained by the CSC - IT Center for Science [19].

3.2 CPPN-NE T Evolutionary lgorithm

CPPN-NEAT has been repeatedly described in detail [24, 5, 4, 12], so we only briefly summarize it here. A Compositional Pattern Producing Network (CPPN) is similar to a neural network, but its nodes contain one of multiple mathematical functions (sine, cosine, Gaussian, sigmoid, linear, square, or positive square root). CPPNs evolve according to the NEAT algorithm, which is largely based on: complexification of genomes over time, speciation within the genotypic space for diversity maintenance, and tournament selection within species [24].

The CPPN produces a spacial output pattern that is built up from these functions' geometric transformations of the input gradients (changing values of each input coordinate over the space). Because the nodes have regular mathematical functions, the output patterns tend to be regular (e.g. a Gaussian function can create symmetry and a sine function can create repetition). In this paper, each voxel has x, y, and z coordinates, polar coordinates (r and) in each of the x, y, and z planes, and a measure of the voxel's distance from the center of the search space (d), which are all input in the range [1, 1], describing the relative location of each voxel in this geometric design space. The single output of this network is interpreted as either a sti material present in that voxel's location for a value above zero, or a soft material present for a value less than or equal to zero.

Alternate experiments were conducted with the value of the output node ([1, 1]) representing a mixture of the sti and soft materials with a compliance representative of an interpolation between the maximally sti or soft materials at each endpoint. While the real valued compliance a ords more flexibility in the design space, the problem of physically mixing materials during the additive manufacturing process is not yet a solved problem [16].

In order to produce a structure from a CPPN, each voxel in the discretized design space is iterated though. At each iteration through this space, the voxel's coordinate are input into the network, which is then undergoes it's update function to produce an output value. The value out this output determines the type of voxel which is placed at this location. A positive output stipulates the placement of a sti voxel (denoted by to a Young's Modulus (E) of 10 gigapascal (GPa), and Poisson's ratio of 0.3), while a negative output value produces a soft voxel at this location (resulting in a Young's Modulus of 1 GPa, and the same Poisson's ratio of 0.3). After iterating through each voxel within the design space, the CPPN genome has produced a phenotypic description of the structure, which can then be analyzed to find it's natural frequencies, or sent to a 3D printer for fabrication. This iterative process is outlined in Fig. 2.

3.3 Fitness Function

The quality (fitness) of each structure's ability to match a desired frequency profile of n frequencies is described by:

$$\frac{1}{\Sigma^{n}_{=1}(\frac{n \quad 1}{n})E(i)^2}$$

Where n is the number of frequencies being optimized, and $E(i)$ is the relative error in matching the i^{t} frequency. The linear weighting factor $\frac{n \ i \ 1}{n}$ is to place more weight on the primary frequencies than the later ones, which contribute less significantly to the behavior of real world systems. For example: for frequency 1 of 10, $\frac{n \ i \ 1}{n} = \frac{10 \ 1 \ 1}{10} = 1$, thus the first frequency contributes to the fitness penalty with a weight of 1. For frequency 6 of 10, this weighting factor becomes $\frac{10 \ 6 \ 1}{10} = 0.5$, so the 6^{t} frequency is discounted such that it's relative error is only counted by half of that be-

longing to the first frequency. Similarly, the 10^t frequency has a discount factor of 0.1, meaning that it's relative error contributes to the overall fitness only one tenth the amount which the error of the 1^{st} frequency does.

The motivation for using the weighted sum of the squared errors is simply a standard practice to negate the sign of the error terms, and to more heavily penalize larger deviations from the desired frequencies.

3.4 Producing Random Target Frequencies

In order to optimize a structure to match a given frequency profile, such a profile must exist within the limits of the structure's realizable material properties. Thus to produce random frequency profiles to be used as targets for the optimization process, we use the following:

$$f_n = \frac{^{\mathbf{sti}}_{n} + ^{\mathbf{soft}}_{n}}{2} + \frac{^{\mathbf{sti}}_{n} - ^{\mathbf{soft}}_{n}}{2} * rand(\ \ 0\,5, 0\,5)$$

For frequency number $n = 1, 2, ..., 10$. Where $f_n^{\mathbf{sti}}$ is the n^t frequency of a beam fully populated with maximally sti voxels (and conversely with soft voxels for $f_n^{\mathbf{soft}}$). Thus the above equation produces a random number from the middle 50% of the range between these minimum and maximum frequencies. Much like the fact that a primary frequency above or below that of the fully sti or soft beams is not physically realizable with the chosen materials, the frequencies at (or near) the edge of this allowable range necessitate beams that are (almost) entirely filled with sti /soft voxels, and thus may or may not be realizable in a case where more than a single frequency is being optimized for. For this proof of concept we conservatively constrain ourselves to the middle 50% of this range, where we feel a balance of both materials is likely to produce a vast array of frequency responses from the relative positions of voxels rather than the proportion of voxel types themselves. Future work will experimentally examine how optimization success drops o as these goals become less and less physically realizable with the expansion of the allowable target frequency range.

After all 10 frequencies are chosen, the values are then sorted from smallest to largest, as natural frequencies must occur in a monotonically increasing order. The 10 target frequencies for four random seeds are given in Fig 3, as well as those of the beams fully populated with sti or soft voxels.

n	Full Soft	Full Sti	Rand. #1	Rand. #2	Rand. #3	Rand. #4
1	0.782	1.596	1.215	1.062	1.044	1.315
2	4.666	9.549	7.994	7.279	6.858	6.613
3	11.973	24.894	18.592	16.059	17.447	19.177
4	12.220	25.087	15.594	17.749	21.404	20.691
5	22.080	45.475	30.026	29.250	33.929	38.461
6	33.513	69.209	49.484	52.985	52.274	49.015
7	35.868	74.574	51.903	59.555	55.862	58.415
8	45.964	95.121	65.639	76.686	59.337	69.871
9	59.072	122.436	84.398	79.505	77.530	97.132
10	59.598	123.911	105.121	87.085	85.164	97.485

Figure 3: The first 10 natural frequencies (in MHz) for beams with all soft voxels or all sti voxels gives the boundaries for the creation of 4 random frequency target profiles (Sec 3.4).

3.5 Control Treatment

In order to test the validity of the evolved structures, a control method was devised. To isolate the e ects of the optimization towards natural frequency matching structures, the control groups consist of the same 32 independent runs of 30 CPPN genomes evolving for 1000 generations. This negates any natural advantage that the genomic representation of the CPPN might have in this domain, as well as the complexification of the NEAT algorithm over time. In the control setup, however, no preferential reproduction is a orded to those individuals who more closely match the desired frequency profile, but rather this selection happens at random. At the end of the 1000 generations of this evolutionary drift, the resulting structure are still compared to each of the four Random Frequency Profiles and their e ectiveness is measured in the same manner as with the experimental treatments.

4. RESULTS

All treatments below consist of 32 independent runs, with populations of 30 individuals evolved for 1000 generations.

4.1 Statistical Measures

The data resulting from the control conditions pass the Shapiro-Wilk test for normality [21] (with $p<0.0329$ for all 10 frequencies), and thus error bars are used to describe this data in the following plots. However, the experimental treatments routinely fail the Shapiro-Wilk test for normality, with many of the 10 frequencies for each random frequency profile falling above the p=0.05 confidence cuto for the normality of the distribution. Given that the shape these distributions are unknown, we employ bootstrapping to produce 95% confidence intervals to graphically describe the experimental data [11]. Given that at least one distribution for any statistical tests will be an experimental treatment, we employ the Mann-Whitney U test, as it does not require the assumption of normality of the data, yet performs almost as well as the student's t-test on normally distributed data (such as the control data) [20].

4.2 Statistical Data

4.2.1 Optimization for Random Frequency Profiles

We optimize the material makeup of our 40x10x1 voxel beam to set its natural frequencies to resonate with Random Frequency Profile #1. This is done for 32 independent trials, using a "soft" material (Young's Modulus(E) of 1 gigapascal(GPa), and Poisson's ratio of 0.3), and a "hard" material (Young's Modulus of 10 GPa, and Poisson's ratio of 0.3) as the material library. We compare the relative error for the task of matching with Random Frequency Profile #1 with the control conditionfor each of the $n = 10$ desired frequencies, resulting in 10 di erent p-values. A one-sided U test is employed in order to test the hypothesis that optimized structures will produce lower errors than the control structures. All of these 10 measures fall below the 95% confidence threshold, as $max(\text{p-values}) < 1.008 * 10^{-5}$, showing statistical significance that our system can e ectively optimize all of the first 10 frequencies of this desired frequency profile.

In order to test the sensitivity of this analysis on this randomly generated target frequency profile, three additional desired frequency sets are randomly produced. These each

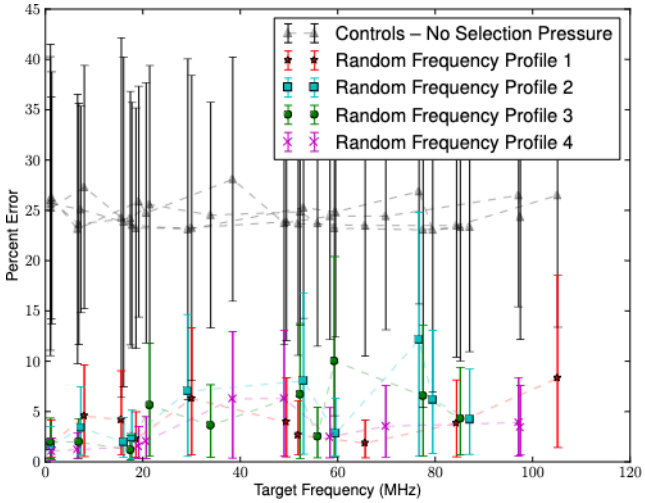

Figure 4: Examination of the e ect of particular random frequency profile targets on the resulting optimization process. Structures are optimized to match (*red stars*) Random Frequency Profile #1, (*blue squares*) #2, (*green circles*) #3, or (*magenta crosses*) #4. While it is not possible to compare the responses to the same frequencies across treatments here, since no two treatments optimize towards the same frequency, we can compare each Random Profile to a control treatment (without selection pressure), plotted as *black triangles*). In all 10 frequencies for all 4 runs, the optimized structures outperform their control counterparts against the same frequencies (with all p-values $< 1.008 * 10^{-5}$), suggesting the ability of this technique to e ectively evolve structures for various frequency profiles.

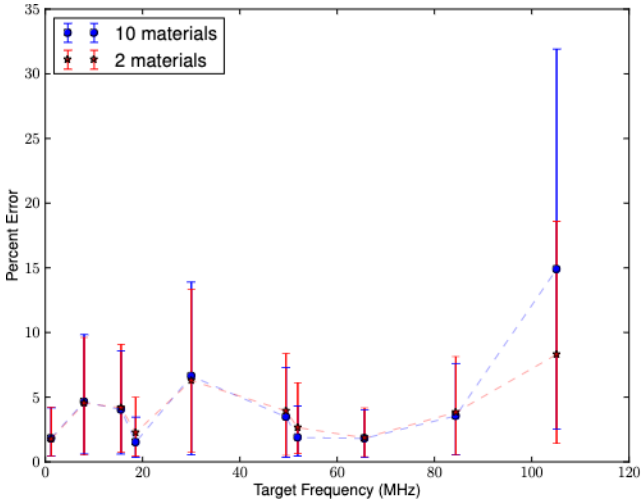

Figure 5: Examination of the e ect of number of materials used on the performance of optimized structures. Both data sets use the same random seeds and target frequency (Random Frequency Profile #1). (*red stars*) Optimized structures from a combination of the maximally sti or maximally soft voxels only (2 materials). (*blue circles*) Each voxel can take on one of 10 intermediate material properties (including the two endpoints in the previous treatment). A two-sided Mann-Whitney U test lacks significant at the 95% confidence level with p-values > 0.0745 for all frequencies except: $n = 4$ (15.594 MHz) with p-value 0.029, and $n = 10$ (105.121 MHz) with p-value 0.0005. This suggests that for most frequencies (besides $n = 4, 10$) the addition of intermediate material properties often does not significantly impact the frequency matching ability of the resulting structures.

consist of $n = 10$ desired natural frequencies, but each of these frequencies di ers from those in Random Frequency Profile #1, so a comparison coupled by desired frequency (in MHz) is no longer possible. One could imagine instead coupling by frequency number, and comparing the accuracy of $n = 1$ for each of the four frequency profiles, then comparing $n = 2$ for all four, and so on. However, actual frequencies between desired profiles can greatly di er: even when comparing with the equivalent frequency number (for example 15.594 MHz for Random Profile #1 is the 4^t desired natural frequency of the system, which has the value 21.404 MHz for Random Profile #3 – a value 37% higher). Additionally, with the highly non-linear nature of the frequency tuning domain, the e ects of di erences in other frequencies may play a major role in the overall structural evolution strategy and influence desired frequencies that do happen to be closely coupled by both n and frequency value (in MHz). Instead, we attempt to compare "apples-to-apples" but assessing each of the optimized structures against control structures evolved through a random walk. These rancom control structures are then compared to the same target frequencies for each of the Random Frequency Profiles. As seen in Fig 4, each of these four independently generated random frequency profiles show a statistically significant improvement over their associated control treatments (with the max p-value of the Mann-Whitney U test $> 1.008 * 10^{-5}$).

4.2.2 *10 Materials vs. 2 Materials*

Fig. 5 shows the e ect of intermediate materials. In this setup, we optimize structures via the same method as in Sec. 4.2, where the CPPN genome specifies the material present in each voxel of the structure by again choosing from one of two materials – either sti (E=10 GPa) or soft (E=1 GPa). To explore the impact of this assumption of two available materials, we compare this to another treatment in which there are 10 material choices, representing materials of intermediate compliances (between and including the endpoints of the fully sti and fully soft voxels as before). Materials 2-9 are assigned a Young's Modulus (E) of 2- 9 GPa, respectively, with a constant Poisson's ratio of 0.3. The results of a two-sided Mann-Whitney U test show that 8 of the 10 desired frequencies showed no significant di erence (min(p-value) > 0.0745. The exceptions to this rule were the frequencies of 15.594 MHz ($n = 4$), which had a p-value < 0.029, and 105.121 MHz ($n = 10$) with p-value < 0.0005. In the case of the final ($n = 10$) frequency of the group, the 10 material structures actually performed worse than their 2 material counterparts. Thus, in general, we believe that using 10 intermediate materials does not typically produce significantly better optimized structures than those made with just the two extreme materials.

Figure 6: Six examples of stereotypical structures evolved for Random Frequency Profile #1. Black pixels represent sti material, while white pixels represent soft material. Optimized structures often consist of one or two large continuous regions. They often span all or nearly all of the design space allocated in both width and length. They also often display minor branching structures o of this primary long-spanning structure.

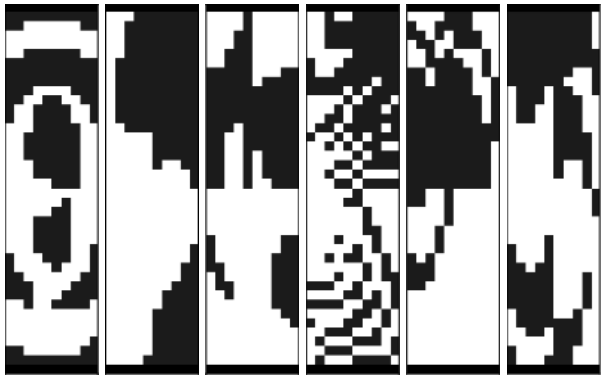

Figure 7: Six examples of stereotypical structures evolved for Random Frequency Profile #2. These structures appear to favor sweeping curvature in their designs, often with repeating or symmetric motifs. This group is shows more use of thinly (or non-)connected areas of sti material than group #1.

Figure 8: Typical structures evolved to match the natural frequencies of Random Frequency Profile #3 display very simple structures with long vertical motifs, often displaying symmetry or repetition along the midpoint of the vertical axis, where a thin strip of sti voxels connects the top and bottom features.

4.2.3 Optimization for the First Natural Frequency

In the course of the work, we also explored other fitness function setups. Of particular interest is the one which rewards only (or disproportionately more) for the matching of the first natural frequency to its desired target. This is of particular interest because the optimization of the first natural frequency alone is considered state of the art in frequency tuning via external damping, and we would like to show that our approach also can be compared directly to traditional approaches. In this case, the following data comes from a quadratic-scaling fitness function. This is a variation on the fitness function described in Sec. 3.3, with the $\frac{n \ \ i \ \ 1}{n}$ term squared, such that the primary natural frequency now accounts for 100 times as much weight as the 10^t natural frequency does (as opposed to 10 times more in the linear scaling scenario above). In this scenario (not plotted here), the 32 independent runs shows a mean of 0.106% error for the primary natural frequency, with a 95% bootstrapped confidence interval of $[0.104\%, 0.110\%]$ error. One could also imagine this trend being even more extreme should the entire weight be placed on the primary frequency.

4.3 Vibrationally Optimized Beam Examples

Fig. 6 shows a representative sample of interesting beams evolved to match Random Frequency Profile #1. The top end has a fixed boundary condition, where the bottom is free; white and black voxels correspond to the soft and sti materials, respectively. These beams tend to feature a long vertical primary structures (or two connected shorter beams spanning the length of the beam), often with horizontal protrusions acting as secondary structures.

Fig. 7 shows beams which are stereotypical of the structures evolved in response to Random Frequency Profile #2. These structures tend to exhibit greater curvature, exhibiting circular patterns from the center of the beam, which presumably rely heavily on the gradients caused by the polar coordinate inputs to the CPPNs. These structures seem more likely than Fig. 6 to include material discontinuities and have multiple floating sections of continuous material instead of a single one than spans the length of the beam.

Figs. 8 and 9 display structures optimized for the remaining target frequency profiles. In Fig. 8, the results of optimization towards Random Frequency Profile #3 display simple vertical structures, often with a repetition or separation point along the mid-line between top and bottom halves of the structures. While in Fig. 9, structures evolved for Random Frequency Profile #4 display a distinct pattern of sti material near the center of the beam, with mostly soft voxels at the top and bottom edges of the structures. These unique structural types, recurring frequently within treatments, but rarely for treatments optimizing towards another random frequency profile, provide further evidence of the algorithm's ability to produce multi-material placements suited for specific vibrational optimization problems.

Alternatively, Fig. 10 showcases the beams created from a process without the selection pressure to optimize towards a specific frequency profile. These structures appear more

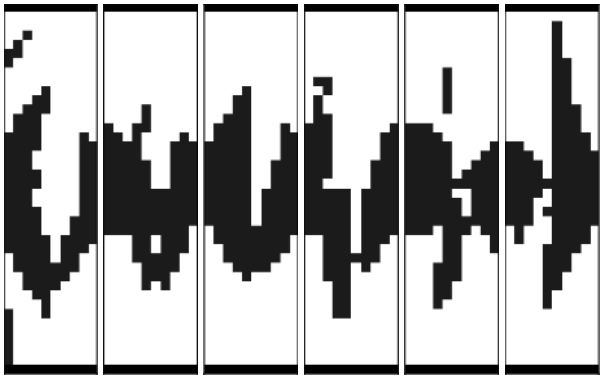

Figure 9: The top six performing structures optimized for Random Frequency Profile #4. This frequency profile tends to drive the evolution of structures with sti voxels concentrated around the center, with near-symmetric "wings" stretching vertically from the primary horizontal structure.

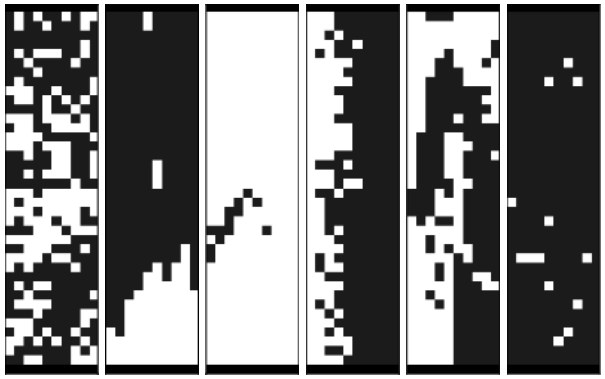

Figure 10: Six examples of stereotypical structures from the control group that features a random walk through the genotypic space in lieu of selection pressure towards high performing structures. The resulting structures appear to be much noisier, with many unconnected single pixels. This suggests that the continuous shapes from the previous trials are preserved because of their vibrational advantages.

pixelated, featuring isolated single, or small groups of, voxels. These structures tend to display very broad divisions, such as a single fuzzy line splitting sti and soft sides of a beam. The presence of these structures implies that the CPPN itself complexifying over time is not in itself sufficient to produce the crisp lines, solid patches, and features such as symmetry and repetition found in Figs. 6-9. But suggests that selection towards specific frequencies, combined with the apparent vibrations benefit of such features for these specific cases, is required to produce these motifs.

4.4 Fabricated Structures

While these structures are evolved in simulation, the optimized beams are easily produced via additive manufacturing. Fig. 11 shows two optimized structures in simulation, and their fabricated counterparts. While the simulated materials in this study were not modeled after any real-world materials, and thus the printed structures were not tested for their actual natural frequencies, future and ongoing work will demonstrate both of these features.

5. DISCUSSION

The above describes a system in which vibrational properties of an existing topological design are optimized through the placement of soft and sti voxels according to an evolved Compositional Pattern Producing Network. The culmination of the results presented previously implies that this new system is indeed capable of producing structures which are optimized to match a predetermined set of natural frequencies. Furthermore, the system is fairly robust to the specific natural frequencies, and their relations to each other – at least within the limited space we explored between range of frequencies existing in single material (all sti or all soft) beams. We compared the results of these beams to those created from a random evolutionary walk to show the ability of the system to optimize for many natural frequencies simultaneously, since there have not existed previous studies which optimize as many as 10 natural frequencies which we could compare our results to. Existing structural optimization methods such as homogenization allow for the optimization of one or few frequencies, but rely heavily on spatially-local gradients or properties which do not capture the highly coupled relationships across a structure that occur when optimizing for multiple frequencies. The employment of an evolutionary algorithm helps to remove the top-down design from this difficult problem, and the use of a CPPN genome creates correlated global mutations which evidently is helpful in optimizing the spacial coupling which made this problem previously unsolvable. In order to compare to the state of the art single frequency optimization, we show that our method can move an object's natural frequency to the order of a tenth of a percent error, without having to a ect it's existing topology or augment it with dampers.

Arguably the most interesting of all, are the examples of optimized topologies in Figs. 6-9. The di erences between the strategies in designing these structures, at such a basic level that it is immediately obvious to the eye, display the flexibility and creativity of design which evolutionary algorithms have previously made their acclaim [2]. The ability to produce structures that are inherently and consistently di erent in their fundamental layout and design strategy, attuned to each new scenario (as opposed to minor variations on a preexisting paradigm) provide the hope that future work with this system will demonstrate the ability to produce e ective and realizable solutions specifically designed for the many real-world applications of vibrational analysis.

6. FUTURE WORK

Given the novelty of this work, the potential for future work is nearly limitless. These authors have begun approaching some of these questions. We are currently upgrading this system to produce 3D structures which include boundary conditions outside of classical beams, running experiments on a larger number of frequencies and on a less restricted set of desired frequency profiles, and exploring the e ect of finer resolution on this design paradigm.

It is also not yet clear how the system will approach demands to push natural frequencies away from wide frequency bands, rather than pushing them towards specific targets (though these two problems are highly related). The fitness

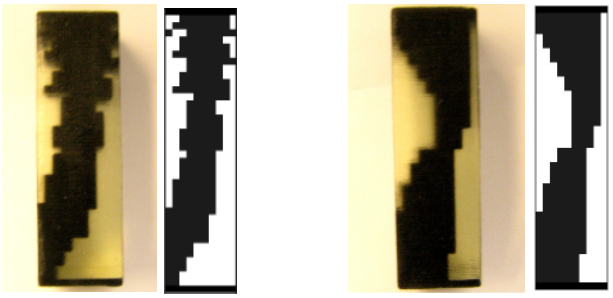

Figure 11: Optimized designs printed on an Objet Connex 500. Shown here are voxels of 0.9mm for visualization purposes, though the resolution on this 3D printer would allow voxels as small as 16 microns.

function employed in this work was chosen logically, though not rigorously, and further experiments will take place to provide evidence of it's e ectiveness in relation to others. Specifically, this applies to multi-objective fitness functions. One could easily imagine other desirable function properties of a real world system, such as the minimization of deflection in a fixed-free beam, which needs to be optimized in parallel with the structures vibrational properties.

Given the ability the system's consistent ability to match all 10 frequencies, it is unknown where the limits of this paradigm fall. In future work, we push this system to failure, exploring its limitations on number of frequencies optimized.

7. CONCLUSION

In this work, we approached the tuning of an object's natural frequencies without the use of external damping or changing the shape envelope of the existing object topology. This problem is of vital engineering importance to produce parts, objects, and structures with are robust to the structural weakening and eventual failures caused by vibrations in many domains such as civil or aerospace engineering. The inverse case is also an important problem, where systems that collect energy and drive oscillations of a piezoelectric beam represent a significant advance in the efficiency of energy harvesting. Despite the difficulty of this problem, we show here that we are capable of producing structures which can optimally place their natural frequencies to match one of multiple desired resonant frequency profiles of 10 frequencies. We do so by optimizing the placement of multiple materials within an existing topology with the evolutionary algorithm CPPN-NEAT. The demonstrated ability to optimize many frequencies simultaneously, as well as the fundamental di erences in structures optimized across multiple target frequency profiles show promise for this technique to soon be a design automation platform for the vibrational optimization of important real-world structures.

8. CKNOWLEDGMENTS

This work was supported by DARPA Open Manufacturnig Grant W911NF-12-1-0449 and NASA Space Technology Research Fellowships NNX13AL37H for Nicholas Cheney and NNX13AL39H for Ethan Ritz.

9. REFERENCES

[1] A. M. Abdel-Gha ar and R. F. Scott. Analysis of earth dam response to earthquakes. *Journal of the Geotechnical Engineering Division*, 105(12):1379–1404, 1979.

[2] P. J. Bentley and D. W. Corne. *Creative evolutionary systems*. Morgan Kaufmann, 2002.

[3] V. R. Challa, M. Prasad, Y. Shi, and F. T. Fisher. A vibration energy harvesting device with bidirectional resonance frequency tunability. *Smart Materials and Structures*, 17(1):015035, 2008.

[4] J. Clune and H. Lipson. Evolving three-dimensional objects with a generative encoding inspired by developmental biology. In *Proc. Conf. Arti cial Life*, pages 144–148, 2011.

[5] J. Clune, K. O. Stanley, R. T. Pennock, and C. Ofria. On the performance of indirect encoding across the continuum of regularity. *IEEE Trans Evol. Comp.*, 15(4):346–67, 2011.

[6] F. E. Culick. Acoustic oscillations in solid propellant rocket chambers. *Astronautica Acta*, 12(2):113–126, 1966.

[7] A. de Ávila Borges, L. Miguel, and L. Miguel. Size and shape optimization of structures by harmony search. 2013.

[8] C. H. Dowding. *Blast vibration monitoring and control*, volume 297. Prentice-Hall Englewood Cli s, 1985.

[9] J. Du and N. Olho . Minimization of sound radiation from vibrating bi-material structures using topology optimization. *Structural and Multidisciplinary Optimization*, 33(4-5):305–321, 2007.

[10] M. B. Dühring, J. S. Jensen, and O. Sigmund. Acoustic design by topology optimization. *Journal of sound and vibration*, 317(3):557–575, 2008.

[11] B. Efron and R. Tibshirani. Bootstrap methods for standard errors, confidence intervals, and other measures of statistical accuracy. *Statistical science*, pages 54–75, 1986.

[12] J. Gauci and K. O. Stanley. Generating large-scale neural nets through discovering geometric regularities. In *Proc. of the Genetic & Evol. Comp. Conf.*, pages 997–1004, 2007.

[13] Z. Hadas, J. Kurfurst, C. Ondrusek, and V. Singule. Ai based optimization for vibration energy harvesting apps. *Microsystem technologies*, 18(7-8):1003–14, 2012.

[14] C. Hales and S. Gooch. *Managing Eng Design*. Springer, 04.

[15] M. Hansen. Improved modal dynamic wind turbines avoid stall-induced vibrations. *Wind Energy*, 6(2):179–95, 2003.

[16] J. Hiller and H. Lipson. Tunable digital material properties for 3d voxel printers. *Rapid Prototyping Journal*, 16(4):241–7, 2010.

[17] C. Q. Howard, C. H. Hansen, and A. C. Zander. Noise reduction of a rocket payload fairing using tuned vibration absorbers with translational and rotational dofs. In *Proc. Australian Acoustical Society*, pages 165–71, 2005.

[18] D. J. Inman. Engineering vibrations. *Prentice-Hall*, 2010.

[19] M. Lyly, J. Ruokolainen, and E. Järvinen. Elmer–a finite element solver for multiphysics. *CSC-report on scienti c computing*, 2000:156–159, 1999.

[20] H. B. Mann and D. R. Whitney. On a test of whether one of two random variables is stochastically larger than the other. *The annals of mathematical statistics*, 18(1):50–60, 1947.

[21] S. S. Shapiro and M. B. Wilk. An analysis of variance test for normality. *Biometrika*, 52(3):591–611, 1965.

[22] D. Shen, J.-H. Park, J. Ajitsaria, S.-Y. Choe, H. C. Wikle III, and D.-J. Kim. The design, fabrication and evaluation of a mems pzt cantilever with an integrated si proof mass for vibration energy harvesting. *Journal of Micromechanics and Microengineering*, 18(5):055017, 2008.

[23] B. K. Stanford and P. D. Dunning. Optimal topology of aircraft rib and spar structures under aeroelastic loads.

[24] K. O. Stanley. Compositional pattern producing networks: A novel abstraction of development. *Genetic Programming and Evolvable Machines*, 8(2):131–162, 2007.

[25] J. Sun, M. R. Jolly, and M. Norris. Passive, adaptive and active tuned vibration absorbers - a survey. *Journal of mechanical design*, 117:234, 1995.

[26] Y. Tarng, J. Kao, and E. Lee. Chatter suppression in turning operations with a tuned vibration absorber. *Journal of materials processing technology*, 105(1):55–60, 2000.